https://doi.org/10.5194/egusphere-2026-2387
Preprint. Discussion started: 17 June 2026

From Fragmentation to Spanning: Connectivity Regime Transitions in Equal-Probability Geohazard Fields

Şahin Çağlar Tuna[1]

[1]Department of Civil Engineering, Yaşar University, İzmir, 35100,Türkiye

Correspondence to: Şahin Çağlar Tuna (tunasahincaglar@gmail.com)

Abstract. Scalar hazard metrics such as exceedance ratio, damaged-area fraction, or marginal failure probability quantify how much of a spatial domain is activated, but they do not determine how that activation is organized. In correlated threshold systems, fields with identical occupation fractions may form fundamentally different connected structures, ranging from dispersed local clusters to dominant domains and system-spanning configurations. This study develops a connectivity-centered framework to examine this non-uniqueness under exact equal-probability conditions. An observed liquefaction manifestation field is used as an empirical reference and transformed into a latent spatial template for controlled coherence experiments. Correlated realizations are generated under prescribed smoothing levels, thresholded to identical occupation fractions, and evaluated using connected-component count, dominant-cluster ratio, fragmentation, cluster concentration, spanning probability, cluster-size hierarchy, and fluctuation-based indicators. The results show that uncorrelated equal-probability fields remain predominantly fragmented, whereas correlated fields can reorganize into clustered, dominant-connected, and spanning states under the same occupation constraint. Regime-occupancy analysis further demonstrates that equal probability does not correspond to a single connected state, but to a coherence-dependent distribution of accessible configurations. Second-largest-cluster and fluctuation analyses indicate that the fragmentation-to-spanning evolution proceeds through mesoscale aggregation and extended transition bands, rather than through a single sharp boundary. Finite-size analyses show that these organizational trends remain structurally interpretable across alternative raster scales. The framework provides a nonlinear geoscience interpretation of thresholded correlated hazard fields, in which spatial coherence acts as a control parameter and connectivity regimes emerge through pattern reorganization under fixed occupation constraints. The study therefore demonstrates that activation extent and spatial organization are distinct system properties, and that connectedness provides an essential descriptor beyond scalar probability alone. More broadly, the framework links correlated random fields, thresholded spatial patterning, null-model contrast, and connectivity-regime transitions for complexity-oriented hazard analysis.

Keywords: Connectivity transitions; Equal-probability fields; Spatial coherence; Regime maps; Fragmentation-to-spanning transition; Correlated spatial systems.

https://doi.org/10.5194/egusphere-2026-2387
Preprint. Discussion started: 17 June 2026

1 Introduction

Scalar hazard metrics such as exceedance ratio, damaged-area fraction, or marginal failure probability describe how much of a spatial domain is activated, but they do not uniquely determine how that activation is arranged. In correlated threshold systems, two fields with the same occupation level may exhibit fundamentally different connected structures, ranging from many dispersed local clusters to dominant domains and system-spanning configurations. Thus, scalar extent alone cannot define the collective state of a spatial system; connectivity and spatial organization must also be considered (Barabási, 1999; Scheffer et al., 2009).

This distinction becomes critical when local states are spatially correlated. Under independent conditions, active cells are governed primarily by the prescribed occupation level. Under correlated conditions, however, neighboring states tend to co-vary, allowing activation to aggregate into connected domains whose geometry depends on the coherence of the underlying field. As a result, similar marginal densities may support very different large-scale patterns and imply different system-level consequences. A field composed of many isolated components and another dominated by a single large connected structure may contain the same occupied fraction, yet represent different organizational states (Saberi, 2015; Barthélemy, 2011; Newman, 2002).

This issue arises across many threshold-driven systems, including percolation processes, ecological occupancy fields, epidemic spread, and spatial hazard domains. However, in hazard analysis, spatial fields are still often interpreted primarily through scalar descriptors of extent or exceedance. Such descriptors are useful, but they do not reveal whether the active domain remains fragmented, becomes clustered, concentrates into a dominant component, or develops domain-scale continuity. The key unresolved issue is therefore not simply whether a given fraction of the domain is activated, but whether equal-probability fields can occupy different connected-state regimes under changing spatial coherence. Similar to other nonlinear geoscience problems in which conventional scalar statistics may obscure hidden organization, spatial hazard fields may contain connectivity structures that are not captured by marginal extent alone. In the present context, the hidden structure is not temporal predictability, but the spatial organization of activation into fragmented, clustered, dominant-connected, or spanning states.

The present study addresses this issue through a connectivity-centered framework for equal-probability hazard fields. The main objective is to determine whether fields constructed under identical occupation constraints can nevertheless reorganize into different connected states as spatial coherence changes. To isolate arrangement from abundance, realizations are generated under controlled coherence conditions, converted to binary fields through exact equal-probability thresholding, and evaluated using connected-component count, dominant-cluster ratio, fragmentation, cluster concentration, spanning behavior, cluster-size hierarchy, and fluctuation-based indicators (Fenton, 1999; Shinozuka and Deodatis, 1996).

https://doi.org/10.5194/egusphere-2026-2387
Preprint. Discussion started: 17 June 2026

Although the framework is formulated in general terms, an observed liquefaction manifestation field is used as an empirical anchor. This provides a physically grounded spatial template while keeping the focus on a broader complexity question: how correlated threshold systems shift from dispersed local activation toward dominant and potentially system-spanning connected forms. In this sense, the geotechnical case supplies the reference geometry, whereas the main contribution lies in the interpretation of connected patterning and regime multiplicity rather than in domain-specific liquefaction prediction (Jayaram & Baker, 2009; Goda & Atkinson, 2010; Wang & Takada, 2005).

The contribution of the study is twofold. Conceptually, it distinguishes activation extent from system-level organization and argues that equal probability does not imply a unique connected state. Methodologically, it develops a controlled framework in which fragmented, clustered, dominant-connected, and spanning forms are treated as alternative connectivity regimes under fixed occupation constraints. The working hypothesis is that the organizational state of an equal-probability field is governed jointly by occupation level and spatial coherence, leading to transition-like behavior and regime multiplicity in correlated spatial systems (Stanley, 1999; Muñoz, 2018).

Accordingly, the objectives of this study are to:

(1) construct a controlled framework for comparing spatial fields under exact equal-probability conditions;

(2) quantify their connected organization using connectivity-based descriptors;

(3) identify how increasing spatial coherence shifts the system from partitioned toward increasingly consolidated states; and

(4) demonstrate that equal-probability fields do not define a unique collective form, but a coherence-dependent set of accessible connectivity regimes.

The remainder of the paper is organized as follows. Section 2 presents the conceptual basis of equal-probability fields, connectivity, and fragmentation-to-spanning transitions. Section 3 describes the computational framework. Section 4 reports the results, including regime evolution, transition bands, null-model comparisons, mesoscale indicators, and robustness analyses. Section 5 discusses the implications for complexity-oriented hazard interpretation, and Section 6 summarizes the main conclusions.

2. Conceptual Framework

2.1. Equal-probability fields and non-unique organization

In this study, an equal-probability field is defined as a binary spatial field in which the marginal occupation or failure fraction is fixed by construction. This constraint ensures that all fields being compared contain the same amount of activated area, thereby isolating spatial organization from abundance. Under this definition, equal probability constrains extent, but leaves the arrangement, connectivity, and hierarchy of occupied cells unconstrained. Different connectivity configurations may therefore arise under the same fixed occupation constraint, reflecting emergent spatial organization rather than abundance itself (Schrenk et al., 2013).

This distinction becomes especially important in correlated media. Under independent conditions, the spatial distribution of active cells is governed mainly by the prescribed occupation level. In correlated systems, however, neighboring states tend to

https://doi.org/10.5194/egusphere-2026-2387
Preprint. Discussion started: 17 June 2026

co-vary, allowing activation to aggregate into organized domains rather than remaining randomly dispersed. Equal-probability fields therefore define not a single collective state, but a set of accessible organizational outcomes whose geometry depends on the coherence structure of the underlying field. This behavior is consistent with the role of long-range correlation and constrained fluctuations in structuring spatial patterns (Torquato, 2018).

From a system perspective, equal probability should therefore be interpreted as a constraint on extent, not as a complete description of state. A highly fragmented field and a nearly spanning field may share the same failed-area fraction while implying very different levels of system-scale consequence. This is consistent with the broader understanding that macroscopic behavior in complex media is controlled not only by phase fraction, but also by the geometry and connectivity of the underlying structure (Ghanbarian et al., 2013).

In the present study, this non-uniqueness is examined within a framework anchored to an observed manifestation geometry. The empirical field provides a reference organizational pattern, whereas the controlled ensemble is used to test how similar occupation levels can reorganize into different connectivity states as spatial coherence changes.

2.2. Connectivity as a descriptor of collective state

To characterize organizational differences among equal-probability fields, this study adopts connectivity as the primary descriptor of collective state. In thresholded spatial fields, the basic units of organization are connected clusters formed by neighboring active or failed cells. These clusters provide a direct representation of how local activation aggregates into larger structures. Their number, relative size, dominance, and domain-scale continuity together define the large-scale connected pattern of the field (Rozenfeld et al., 2008).

Within this perspective, several connectivity descriptors become especially relevant. The number of connected components measures the degree of partitioning and provides a direct indicator of fragmentation. The largest connected component ratio captures the extent to which active cells are concentrated within a dominant structure. The concentration of occupied mass within the largest few clusters provides additional information on organizational hierarchy, distinguishing distributed patch structures from fields controlled by a small number of major components. Finally, spanning behavior indicates whether a connected structure extends across the domain, marking the emergence of system-scale continuity (Balberg et al., 1984; Sahimi, 1994).

These descriptors are not used only as geometric summaries. In the present framework, they provide the operational basis for identifying collective connectivity states. A highly partitioned field, a hierarchically clustered field, a dominant-component field, and a spanning field represent different modes of organization. Connectivity therefore functions as a system-level indicator of whether local activation remains localized or reorganizes into broader collective structure. This interpretation is consistent with graph-based and percolation-oriented views of complex systems, in which connectedness is closely related to emergent regime behavior (Cohen et al., 2000; Callaway et al., 2000).

https://doi.org/10.5194/egusphere-2026-2387
Preprint. Discussion started: 17 June 2026

2.3. From fragmentation to spanning as a regime problem

The fragmentation-to-spanning evolution is interpreted here as a regime problem rather than as a simple monotonic increase in occupied fraction. Under low coherence, equal-probability fields are expected to remain highly partitioned, with activity distributed among many small isolated clusters. As coherence increases, neighboring cells become more likely to share the same state, allowing small components to merge into fewer and larger structures. With further coherence increase, dominant connected components may emerge and, under suitable occupation conditions, develop into spanning configurations that connect opposite sides of the domain (Achlioptas et al., 2009; Ziff, 2010).

This progression defines a sequence of organizational regimes. A fragmented regime is characterized by many disconnected components and the absence of dominant connectivity. A clustered regime reflects partial aggregation, in which the field remains discontinuous but begins to organize into larger structures. A dominant-connected regime emerges when a substantial share of the active domain becomes concentrated within a single major component. A spanning regime is reached when connectedness extends across the domain and the field acquires system-scale continuity. These regimes are not merely visual categories; they represent qualitatively distinct collective states with different system implications (Dorogovtsev et al., 2001).

Within this interpretation, the system state is governed jointly by occupation level and spatial coherence. Occupation controls the amount of activated area, whereas coherence controls how that activated mass is redistributed into connected structures. Spanning is therefore not simply the endpoint of increasing abundance; it marks the emergence of domain-scale connectivity when both occupation and coherence support large-scale organization. The conceptual aim of the study is to identify these organizational states and examine how they emerge under controlled equal-probability conditions.

The present work therefore treats fragmentation-to-spanning behavior as an organizational transition problem examined through the joint use of observed hazard geometry and controlled coherence experiments. In this framework, coherence acts as a control parameter, while the dominant-cluster ratio Γ behaves as an order-parameter-like indicator of large-scale structural concentration. The regime sequence from fragmentation to spanning thus represents a structured evolution of connected-state classes under fixed scalar constraints.

3. Computational Framework

3.1. Empirical basis and spatial representation

The computational framework was designed to combine real-data grounding with controlled system experimentation. It consists of three complementary stages: direct connectivity analysis of the observed liquefaction manifestation field, construction of a coherence-controlled ensemble from an empirical latent template, and post-processing for regime-threshold refinement and representative realization selection. This structure allows the observed field to provide the empirical reference geometry, while the controlled ensemble isolates the effect of spatial coherence under fixed occupation conditions.

The starting point was an observed liquefaction manifestation dataset in which each record contained spatial coordinates and a manifestation descriptor. The descriptors were parsed into a binary indicator denoting the presence or absence of

https://doi.org/10.5194/egusphere-2026-2387
Preprint. Discussion started: 17 June 2026

liquefaction manifestation at each location. To enable spatial connectivity analysis, the point observations were projected onto a regular two-dimensional lattice with a grid spacing of 250 m in both horizontal directions. Each observation was assigned to its nearest grid cell; when multiple observations occupied the same cell, manifestation presence dominated so that the cell state reflected the occurrence of manifestation at that location. This procedure produced a binary occupancy field representing the observed manifestation pattern over the study domain (Cressie, 1993). The resulting grid served both as the support for direct connectivity analysis and as the spatial basis for the controlled coherence experiments.

The observed binary field was first analyzed directly to establish its empirical connectivity signature. Occupied cells were treated as active sites on a regular lattice, and connected components were identified using a four-neighbor definition, in which horizontal and vertical adjacency determined component membership (Hoshen & Kopelman, 1976; Newman & Ziff, 2001). For the observed field, the computed descriptors included the number of connected components, largest connected component size, dominant-cluster ratio, fragmentation index, top-3 cluster ratio, spanning indicator, cluster entropy, and a susceptibility-like metric derived from the component-size spectrum (Stauffer, 1979; Christensen & Moloney, 2005).

The dominant-cluster ratio was defined as

$$\Gamma = \frac{|C_{max}|}{|D_a|} \tag{1}$$

where |Cmax| is the size of the largest connected component and |Da| is the total number of occupied cells. The fragmentation index was defined as

$$FI = \frac{N_c}{|D_a|} \tag{2}$$

where Nc is the number of connected components. Larger FI values indicate a more partitioned active domain relative to its total occupied extent. The top-3 cluster ratio was computed as the fraction of occupied cells contained in the three largest connected components.

A left-to-right spanning criterion was adopted for the observed-field analysis to avoid overly permissive spanning classification. Under this definition, a field was classified as spanning only if at least one connected component linked the left and right boundaries of the domain (Ziff, 1992). The purpose of this stage was to establish the empirical connectivity structure of the observed manifestation field, which then served as the reference state for the latent-template construction and controlled coherence experiments.

3.2. Construction of the controlled equal-probability ensemble

In the second stage of the framework, the observed binary manifestation field was converted into a continuous latent template for controlled coherence experiments. The purpose of this step was to preserve the broad empirical organization of the observed field while allowing spatial coherence to be varied systematically. The binary field was smoothed using a light Gaussian filter to generate a continuous latent intensity surface, which was then normalized to the unit interval and used as

https://doi.org/10.5194/egusphere-2026-2387
Preprint. Discussion started: 17 June 2026

the empirical organizational substrate of the study (Rasmussen & Williams, 2006; Stein, 1999). This latent template should not be interpreted as a direct physical intensity measure, such as factor of safety or pore-pressure ratio. Rather, it represents a real-data-informed spatial tendency field derived from the observed manifestation geometry.

Controlled realizations were generated by combining stochastic perturbation with coherence filtering. For each realization, a spatial noise field was added to the latent template, and the perturbed field was smoothed using a Gaussian filter with prescribed coherence parameter σc. The parameter σc acted as the control variable governing the smoothness and spatial continuity of the resulting field. A set of coherence scenarios was defined, ranging from weakly organized to strongly coherent conditions. For each coherence level, multiple independent realizations were generated, forming a Monte Carlo ensemble of possible organizational states (Fishman, 1996). The continuous fields were normalized to the unit interval before thresholding to preserve comparability across scenarios.

To isolate organization from abundance, each continuous realization was converted into a binary field using exact equal-probability thresholding. Instead of applying a common absolute threshold across realizations, a realization-specific quantile threshold was selected so that the final occupied fraction matched a prescribed target probability exactly.

For a realization $X^{(k)}(s)$, the binary field $I^{(k)}(s)$ is defined as

$$I^{(k)}(s) = \begin{cases} 1, & if\ X^{k}(s) > T^{(k)} \\ 0, & otherwise \end{cases} \quad (3)$$

where $T^{(k)}$ denotes the realization-specific quantile threshold. The occupied fraction of the binary field is then given by:

$$p^{(k)} = \frac{1}{M}\sum_{i=1}^{M} {I_i}^{(k)} \quad (4)$$

where M is the total number of grid cells in the spatial domain, and ${I_i}^{(k)}$ represents the binary state of the i-th cell in realization k. By construction, $P^{(k)}$ was made equal to the prescribed target occupation probability for every realization within a given scenario. This step is central to the framework because it allows changes in connectivity to be attributed to coherence-driven spatial reorganization rather than to changes in activated area.

3.3. Connectivity metrics and ensemble-based organization

Each thresholded realization was interpreted as a spatial connectivity system on a two-dimensional lattice. Connected components were identified using the same four-neighbor rule adopted for the observed field. For every realization, a consistent set of descriptors was computed, including the number of connected components Nc, largest connected component size, dominant-cluster ratio Γ, fragmentation index, top-3 cluster ratio, spanning indicator, cluster entropy, and a susceptibility-like measure derived from the component-size distribution.

https://doi.org/10.5194/egusphere-2026-2387
Preprint. Discussion started: 17 June 2026

The spanning indicator was evaluated using a strict left-to-right criterion, because exploratory analyses showed that more permissive definitions led to excessive spanning classification. Together, these descriptors provide a multi-scale characterization of spatial structure. Nc and the fragmentation index quantify partitioning, Γ and the top-3 cluster ratio quantify concentration and dominance, the cluster-size distribution describes hierarchical organization, and spanning behavior identifies the emergence of domain-scale connectivity (Christensen & Moloney, 2005).

Beyond summary descriptors, the full connected-cluster size distribution was extracted for each realization. Complementary cumulative distribution functions were constructed for selected scenarios to visualize how the cluster hierarchy evolves with increasing coherence. A susceptibility-like measure was also computed from the component-size distribution after excluding the largest component, allowing intermediate organizational states to be detected before full consolidation into a dominant structure. It was defined as

$$X = \frac{\sum_{i \neq i_{max}} |C_i|^2}{\sum_{i \neq i_{max}} |C_i|} \quad (5)$$

where $|C_i|$ is the size of the i-th connected component and i_{max} denotes the largest connected component, which is excluded from the summation. This definition emphasizes the contribution of finite non-dominant clusters and is therefore useful for detecting mesoscale organization within the transition band. These quantities are important because fragmentation-to-spanning behavior cannot be characterized adequately by mean descriptors alone; the redistribution of connected mass across scales provides direct evidence of structural reorganization.

For each coherence–occupation combination, ensemble statistics were computed across realizations. These included the mean values of Nc, Γ, fragmentation index, top-3 ratio, entropy, susceptibility, and spanning probability. In addition, fluctuation measures, including the variances of Γ, Nc, and spanning behavior, were evaluated to identify transition-sensitive regions of the parameter space, consistent with fluctuation-based approaches used in finite-size scaling analysis of statistical systems (Binder, 1981). Percentile-band summaries were also constructed for key descriptors to quantify realization-to-realization variability.

Based on these ensemble descriptors, each coherence–occupation combination was classified into one of four organizational regimes: fragmented, clustered, dominant connected, or spanning. Because preliminary classification tended to over-identify spanning states, a post-processing calibration stage was applied to refine the regime boundaries. The regime map presented in the Results section is therefore based on these stabilized thresholds.

Representative realizations were then selected to illustrate characteristic organizational states under equal-probability conditions. These selections were made through a structured post-processing procedure to ensure consistency with the ensemble statistics: low-coherence cases emphasize fragmented structures, intermediate cases reflect clustered organization, and high-coherence cases exhibit dominant or near-spanning connectivity. These realizations serve as visual counterparts to the statistically defined regimes.

Finally, three additional analyses were introduced to strengthen the system-level interpretation. First, a null-model comparison was performed by generating equal-probability fields without imposed spatial coherence, allowing correlation-

https://doi.org/10.5194/egusphere-2026-2387
Preprint. Discussion started: 17 June 2026

driven organization to be isolated explicitly. Second, regime-occupancy probabilities were computed for each coherence–occupation combination, so that the system could be interpreted through the distribution of fragmented, clustered, dominant-connected, and spanning outcomes rather than through ensemble means alone. Third, mesoscale aggregation was quantified using the second-largest cluster fraction and associated fluctuation peaks. Together, these analyses assess whether correlation changes only descriptor values or also the range of accessible connected states under fixed coherence–occupation constraints.

4. Results

4.1. Empirical anchor and coherence-controlled reorganization

The connectivity analysis was first applied to the observed liquefaction manifestation field to establish the empirical reference state of the study. The binary manifestation map shows a clustered and non-uniform pattern rather than a uniformly connected manifestation domain, with a dominant manifested region embedded within smaller disconnected satellite clusters (Figure 1). This indicates that the observed manifestation field already possesses internal organization beyond simple areal extent.

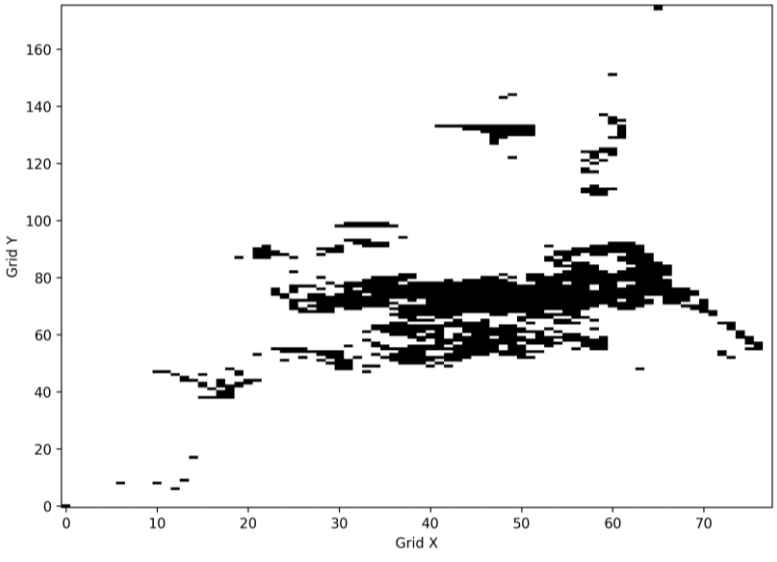

Figure 1: Observed liquefaction manifestation field represented as a binary occupancy map.

The connected-component decomposition confirms this interpretation. As shown in **Figure 2**, one major connected component occupies a substantial share of the observed manifested domain, while many smaller components remain distributed around it. The field is therefore not purely fragmented, but neither does it collapse into a single system-wide connected structure. In other words, the empirical manifestation pattern already exhibits the kind of mixed organization that motivates the present framework: substantial extent does not imply a unique connectivity state (Urban et al., 2009).

https://doi.org/10.5194/egusphere-2026-2387
Preprint. Discussion started: 17 June 2026

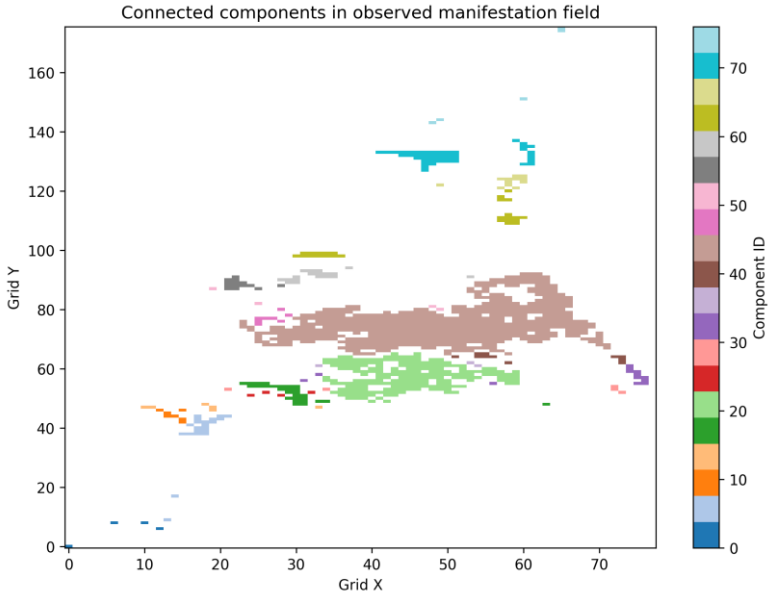

Figure 2: Connected-component decomposition of the observed manifestation field.

The observed cluster-size hierarchy further supports this interpretation. The CCDF shown in Figure 3 exhibits a strongly right-skewed component-size distribution, with many small clusters and only a limited number of large connected components. This pattern indicates hierarchical organization rather than uniform partitioning and characterizes the observed field as a dominant-connected structure accompanied by multiple disconnected secondary clusters (Clauset et al., 2009).

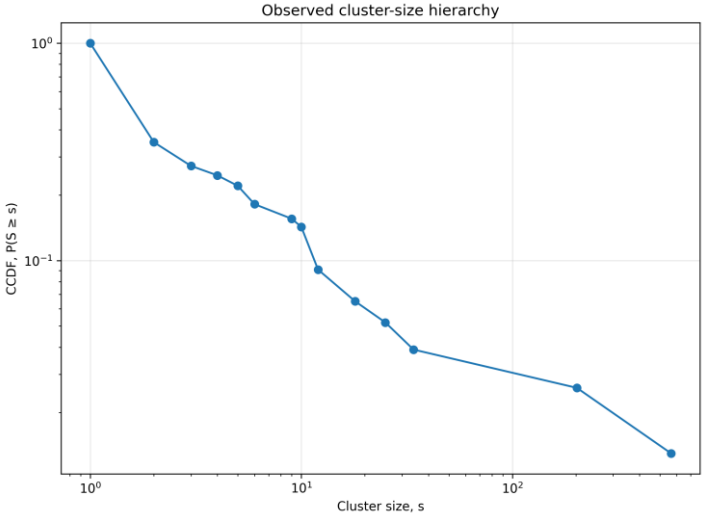

Figure 3: Cluster-size hierarchy of the observed manifestation field expressed as the complementary cumulative distribution P(S≥s) on log–log axes.

https://doi.org/10.5194/egusphere-2026-2387
Preprint. Discussion started: 17 June 2026

280 To further clarify the internal structure of the observed field, the largest connected component was extracted separately (**Figure 4**). This component occupies a substantial share of the manifested domain, yet it does not span the full study area under the adopted left-to-right criterion. The observed field therefore combines dominant connectedness with residual fragmentation rather than collapsing into a single system-wide connected state.

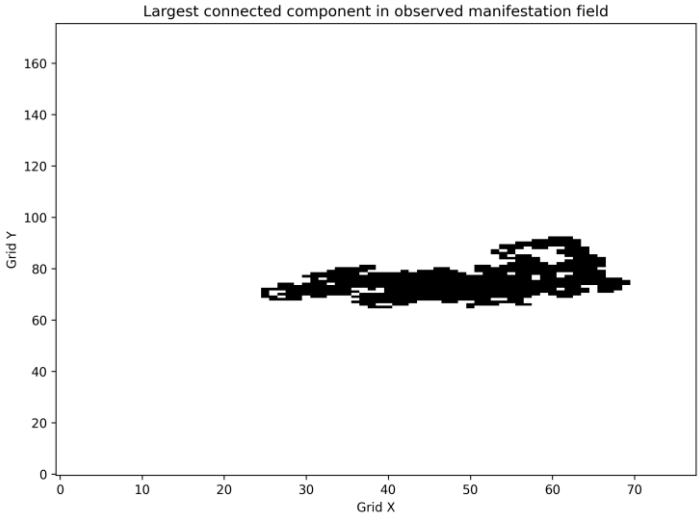

285 **Figure 4: Largest connected component extracted from the observed manifestation field.**

Taken together, **Figures 1–4** provide the empirical basis of the study. The observed manifestation field therefore serves as the real-data reference state for the controlled coherence ensemble introduced below. It already shows that hazard extent alone is insufficient, because a single empirical pattern may simultaneously contain dominant connectedness and residual fragmentation (Turner, 1989).

290 The controlled coherence experiments show a systematic reorganization of the latent field as spatial coherence increases. In the representative continuous fields, low coherence produces short-scale irregularity and fine spatial heterogeneity, whereas higher coherence generates broader and smoother spatial domains (Figure 5). Because the fields are shown before equal-probability thresholding and are normalized to the same unit interval, the figure illustrates the effect of the coherence parameter on spatial organization rather than differences in occupation level.

https://doi.org/10.5194/egusphere-2026-2387
Preprint. Discussion started: 17 June 2026

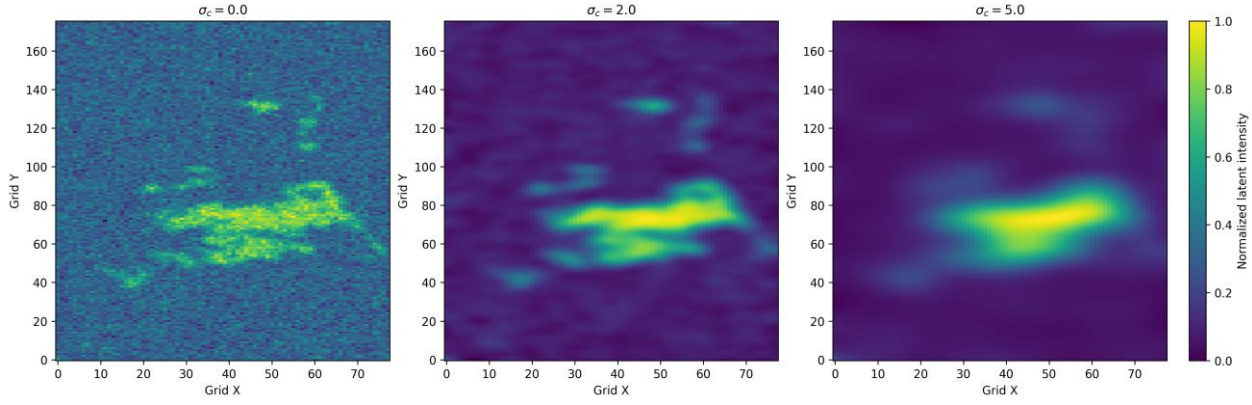

Figure 5: Representative coherence-controlled continuous latent fields before equal-probability thresholding.

After exact equal-probability thresholding, this reorganization becomes visible in the connectivity metrics. Figure 6 shows that the number of connected components decreases sharply with increasing coherence for all occupation levels. The strongest decline occurs between the lowest and intermediate coherence conditions, indicating that the system rapidly reorganizes away from a highly partitioned state once local correlation becomes sufficiently strong (Keitt et al., 1997).

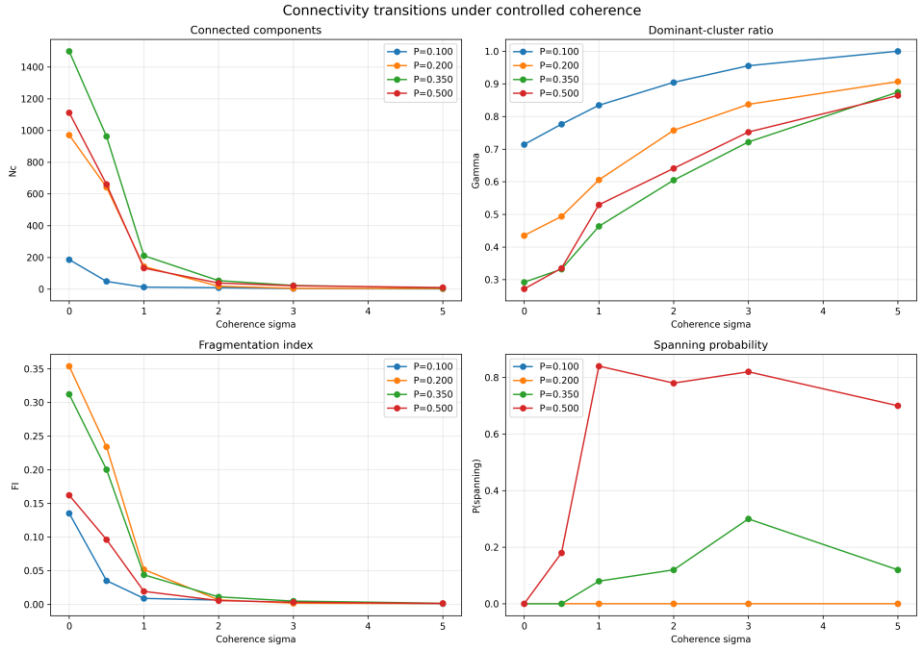

Figure 6: Connectivity transitions under controlled coherence for different target occupation probabilities.

A complementary trend is observed in the dominant-cluster ratio. As summarized in **Table 1**, this ratio generally increases with coherence, demonstrating that progressively larger fractions of the active domain become concentrated within a

https://doi.org/10.5194/egusphere-2026-2387
Preprint. Discussion started: 17 June 2026

dominant connected structure. In parallel, the fragmentation index decreases systematically, confirming that the reduction in component count reflects structural consolidation rather than a purely numerical change in cluster labeling (With et al., 1997). Spanning behavior shows a more conditional response. It becomes possible, and often highly probable, when sufficient occupation and coherence occur together, although its response is not strictly monotonic across all coherence levels. Lower occupation levels more often remain dominant-connected without developing full domain-scale continuity. These results indicate that spanning is not controlled by coherence alone; rather, it emerges through the combined effect of occupation level and correlation-driven organization (He & Hubbell, 2003).

Table 1: Simplified ensemble connectivity summary for representative coherence–occupation combinations.

σc	P	Mean N_c	Mean Γ	P(spanning)	Mean Susceptibility	Regime
0	0.1	185.8	0.714	0	13.6	Dominant connected
1	0.1	12.1	0.834	0	31.1	Dominant connected
5	0.1	1.1	1	0	1290.7	Dominant connected
0	0.35	1499.6	0.292	0	14.6	Clustered
1	0.35	210.5	0.463	0.08	95.3	Dominant connected
5	0.35	7.5	0.874	0.12	329.7	Dominant connected
0	0.5	1112.6	0.271	0	35.4	Clustered
1	0.5	132	0.529	0.84	192.4	Spanning
5	0.5	9.7	0.864	0.7	223.5	Spanning

Overall, Figure 5, Figure 6, and Table 1 demonstrate that increasing coherence drives a genuine connectivity transition: the system generally moves from partitioned multi-cluster organization toward progressively more concentrated, dominant, and, under favorable occupation conditions, spanning states. Thus, coherence does not merely smooth the latent field; it reorganizes the thresholded system into structurally different connectivity states (Pascual & Guichard, 2005).

4.2. Equal probability, connectivity hierarchy, and dominant-structure emergence

The realization-level effect of equal-probability thresholding is illustrated for P=0.35 under three coherence levels **(Figure 7).** Since the occupied fraction is fixed by construction, the visual and metric differences among these fields reflect changes

https://doi.org/10.5194/egusphere-2026-2387
Preprint. Discussion started: 17 June 2026

in connectivity organization rather than changes in activated area. This comparison therefore isolates the role of coherence in reorganizing the same occupied mass into different connected forms.

At low coherence, activation is distributed among many small disconnected clusters, producing a highly partitioned configuration. Although the total occupied fraction is the same as in the other panels, the active cells remain spatially dispersed and only weakly consolidated. At intermediate coherence, cluster merging becomes evident: the number of disconnected components decreases, and larger connected structures begin to form. At high coherence, the active domain is reorganized into a small number of large components. This progression is reflected directly by the decrease in Nc and the increase in Γ, indicating a transition from partitioned organization toward dominant connected structure.

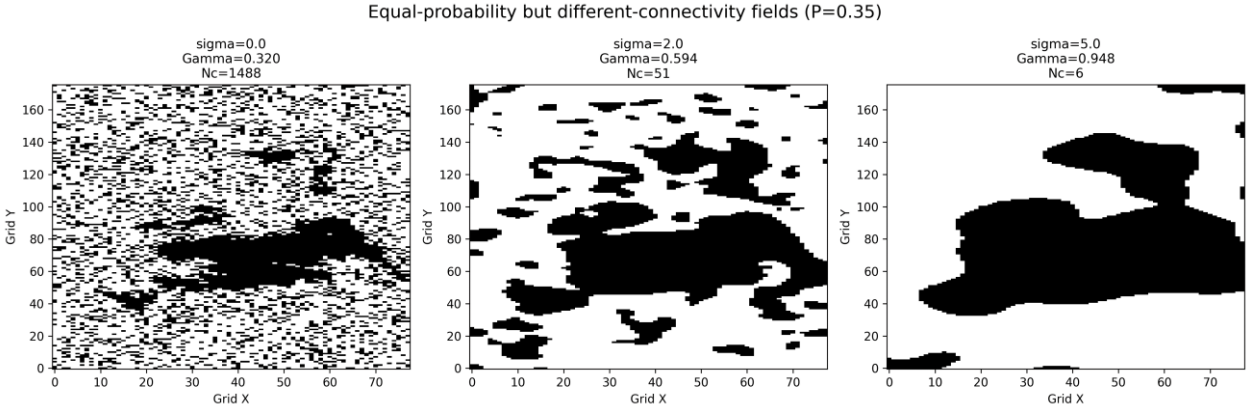

Figure 7: Representative equal-probability binary fields under selected coherence levels (P=0.35).

This realization-level comparison is important because it shows that equal probability does not merely allow small metric fluctuations around a common pattern. Instead, fields with the same occupation fraction can occupy visibly different connected configurations as coherence changes. The same scalar constraint therefore produces different spatial organizations when the correlation structure of the underlying field is altered.

A more detailed view of this reorganization is obtained from the cluster-size hierarchy. **Figure 8** presents the ensemble cluster-size hierarchy under the same equal-probability condition (P=0.35) for selected coherence levels. Under weak coherence, the distribution declines rapidly, indicating that occupied mass remains dispersed across many small clusters. As coherence increases, the distribution develops a longer upper tail, showing that larger connected components become progressively more prominent.

https://doi.org/10.5194/egusphere-2026-2387
Preprint. Discussion started: 17 June 2026

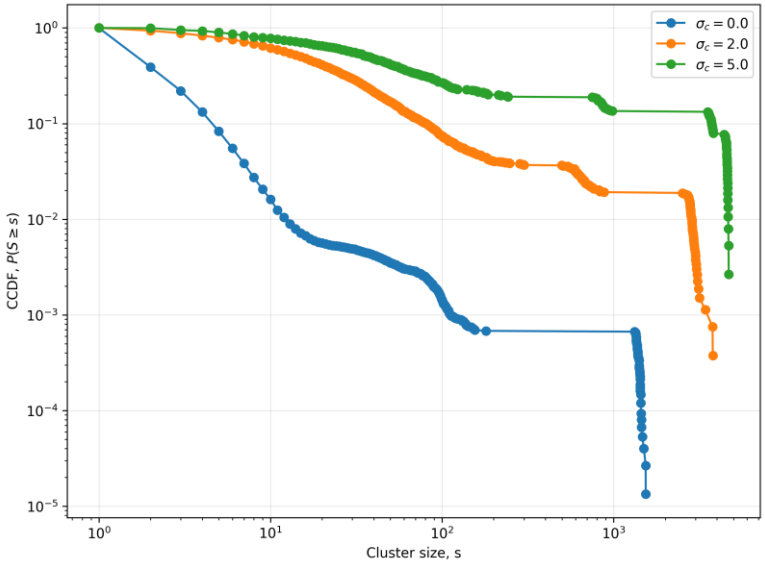

Figure 8: **Ensemble cluster-size hierarchy under equal-probability conditions (P=0.35), expressed as the complementary cumulative distribution P(S≥s) for selected coherence levels.**

The broadening of the upper tail indicates that the transition is not a simple smoothing effect. Rather, coherence redistributes occupied mass across the component hierarchy. Small clusters become less dominant in the overall structure, while intermediate and large components account for an increasing share of the occupied domain. This hierarchical aggregation provides the mechanism by which partitioned configurations evolve toward dominant connected forms.

Accordingly, the combination of representative fields and cluster-size hierarchies shows that the equal-probability transition is driven by redistribution of connected mass across the cluster hierarchy rather than by a change in occupied fraction. This establishes the structural basis for the ensemble-level transition-band and regime analyses presented in the next section.

4.3. Transition bands and regime structure

Mean trends alone do not fully describe the fragmentation-to-spanning evolution. The ensemble results also show systematic changes in variability, indicating that some coherence–occupation combinations are more transition-sensitive than others. **Figure 9** presents the variance of Γ, the variance of spanning behavior, and the mean susceptibility across coherence levels.

https://doi.org/10.5194/egusphere-2026-2387
Preprint. Discussion started: 17 June 2026

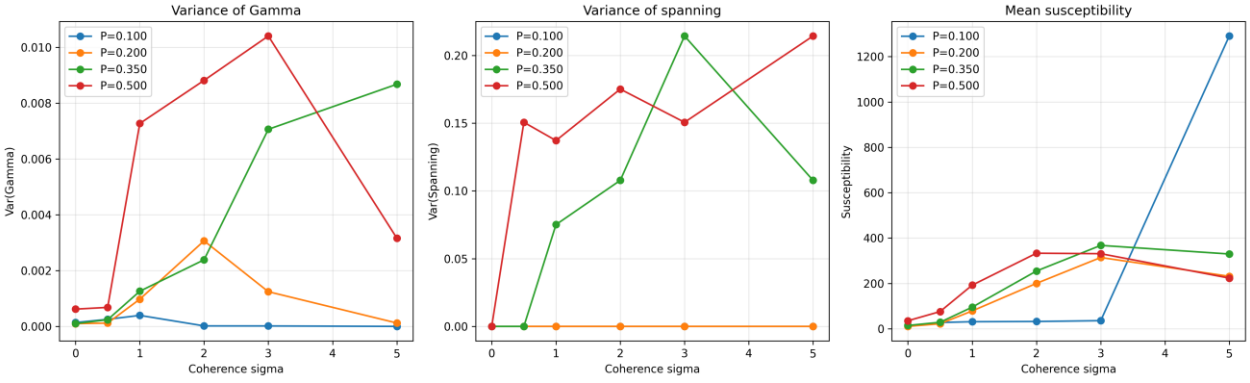

Figure 9: **Variability and susceptibility responses across coherence levels.**

The fluctuation patterns show that variability is concentrated in specific regions of the coherence space rather than being uniform. At low coherence, the system is generally partitioned into many components, whereas increasing coherence promotes the formation of larger connected structures. Intermediate coherence levels often exhibit elevated variability, reflecting competition among clustered, dominant-connected, and near-spanning outcomes under the same scalar constraints. This supports the interpretation of the transition as an extended band of organizational instability rather than a single abrupt threshold.

The susceptibility response provides complementary evidence for this transition-zone behavior. In several occupation regimes, susceptibility increases before declining or stabilizing, indicating the temporary presence of substantial finite-cluster organization. This suggests that the system passes through a mesoscale aggregation stage before large-scale consolidation becomes dominant.

The percentile-band evolution in **Figure 10** further supports this interpretation. The dominant-cluster ratio Γ increases systematically with coherence, while Nc decreases sharply, confirming the progressive consolidation of occupied cells into fewer and larger connected structures. The widening of the percentile bands in intermediate coherence ranges indicates elevated realization-to-realization variability, consistent with a transition zone in which alternative organizational outcomes remain accessible. The susceptibility response further shows that finite-cluster organization can remain important before dominant or spanning configurations are fully established.

https://doi.org/10.5194/egusphere-2026-2387
Preprint. Discussion started: 17 June 2026

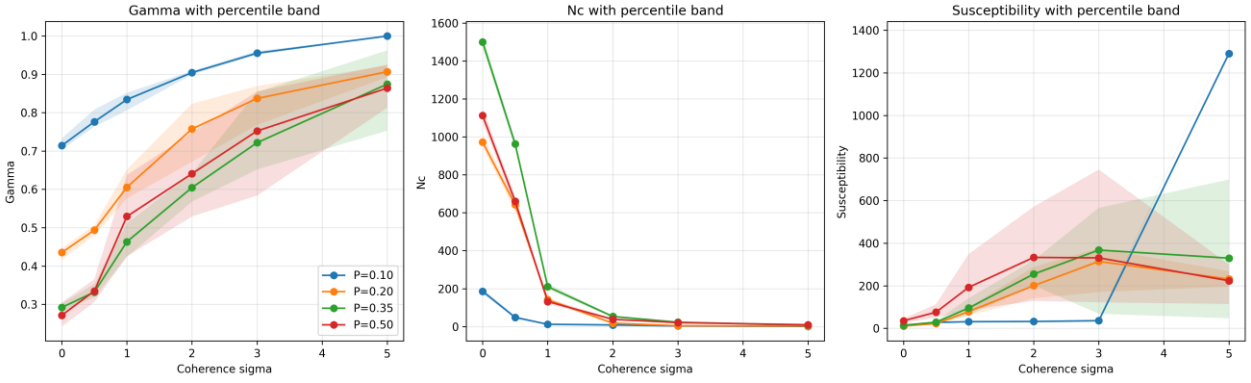

Figure 10: **Ensemble percentile-band evolution of Γ, Nc, and susceptibility-like finite-cluster response across coherence levels.**

When the ensemble-averaged descriptors and fluctuation-based indicators are considered together, the coherence–occupation plane can be interpreted as a regime map. The recalibrated map in **Figure 11** shows that different combinations of target occupation probability and coherence correspond to different organizational states.

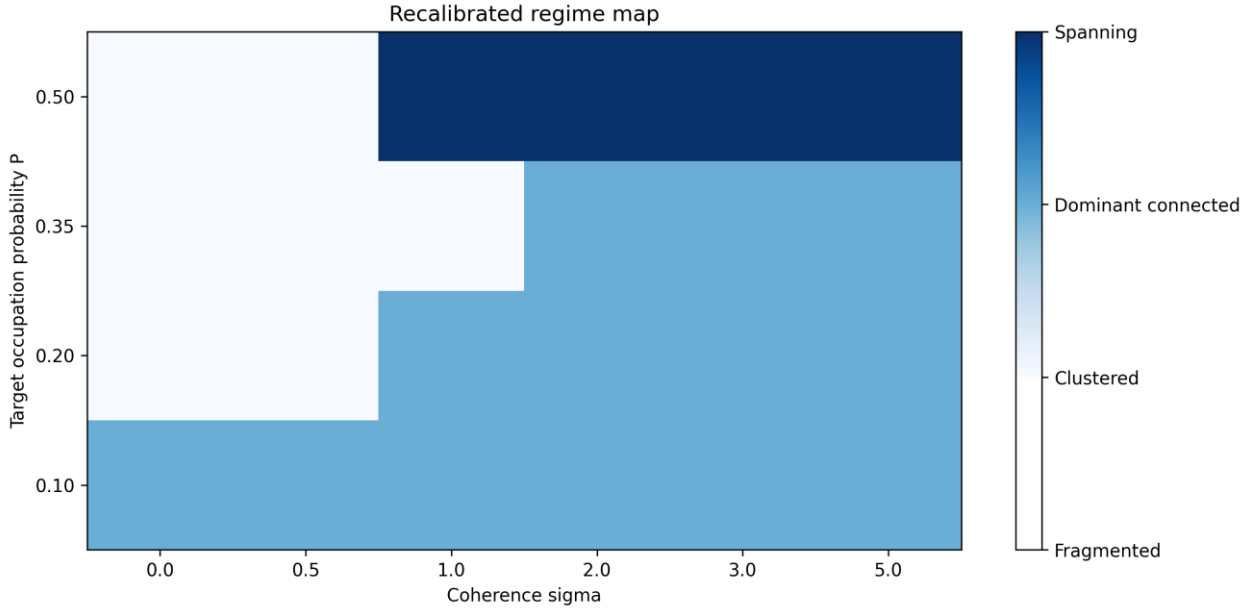

Figure 11: Recalibrated regime map in the coherence–occupation parameter space.

At lower occupation levels, the system tends to remain clustered or dominant-connected across much of the coherence range. At intermediate occupation levels, increasing coherence progressively shifts the field toward more consolidated connected states. At the highest occupation level considered here, spanning becomes the dominant regime once coherence exceeds the

https://doi.org/10.5194/egusphere-2026-2387
Preprint. Discussion started: 17 June 2026

lower range. Thus, the regime boundaries are controlled jointly by occupation level and spatial coherence rather than by either parameter alone.

The regime map also clarifies that spanning is not simply a stronger form of clustering. It represents a distinct organizational state in which connectedness becomes domain-scale. Similarly, clustered and dominant-connected fields occupy different positions within the transition sequence: the former reflects partial aggregation, whereas the latter indicates concentration of occupied mass into a major connected component. Overall, Figures 9–11 show that the connectivity transition is expressed not only through changes in mean descriptors, but also through fluctuation bands, percentile spreads, and regime shifts in the coherence–occupation plane.

4.4. Null-model comparison and state multiplicity

To determine whether the observed reorganization is genuinely correlation-driven, a null-model comparison was performed using equal-probability fields without imposed spatial coherence. **Figure 12** compares the correlated and uncorrelated ensembles in terms of the dominant-cluster ratio Γ, mean connected-component count Nc, spanning probability, and susceptibility-like finite-cluster response. The contrast is clear: uncorrelated fields remain effectively fragmented, with very low Γ, high Nc, negligible spanning probability, and weak susceptibility response. By contrast, correlated fields show systematic concentration into dominant connected forms, sharp reductions in Nc, non-zero spanning probabilities at intermediate-to-high occupation levels, and stronger finite-cluster susceptibility.

https://doi.org/10.5194/egusphere-2026-2387
Preprint. Discussion started: 17 June 2026

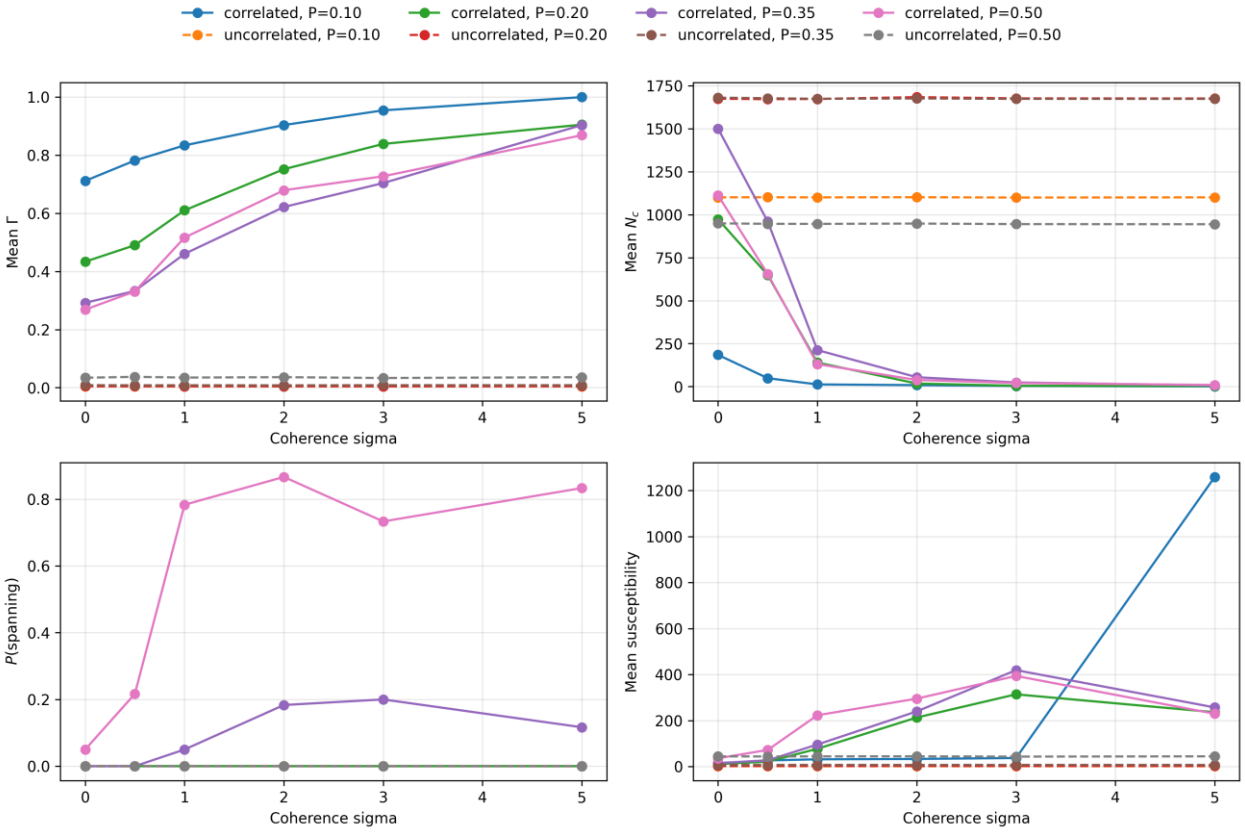

Figure 12: Correlated versus uncorrelated equal-probability ensembles.

These results show that the transition sequence is not generated by occupied fraction alone. Under the same equal-probability constraint, the uncorrelated ensemble remains highly partitioned, whereas the correlated ensemble reorganizes into dominant-connected and, at higher occupation levels, spanning states. Thus, the connectivity transition requires spatial correlation rather than merely a fixed amount of occupied area.

The effect of correlation is not limited to changes in ensemble-mean descriptors. It also alters the distribution of connectivity regimes accessible to the system. **Figure 13** presents the regime-occupancy probabilities for the correlated ensemble. Several coherence–occupation combinations exhibit non-trivial mixtures of clustered, dominant-connected, and spanning outcomes, indicating that the system does not occupy a single deterministic state under fixed scalar constraints.

https://doi.org/10.5194/egusphere-2026-2387
Preprint. Discussion started: 17 June 2026

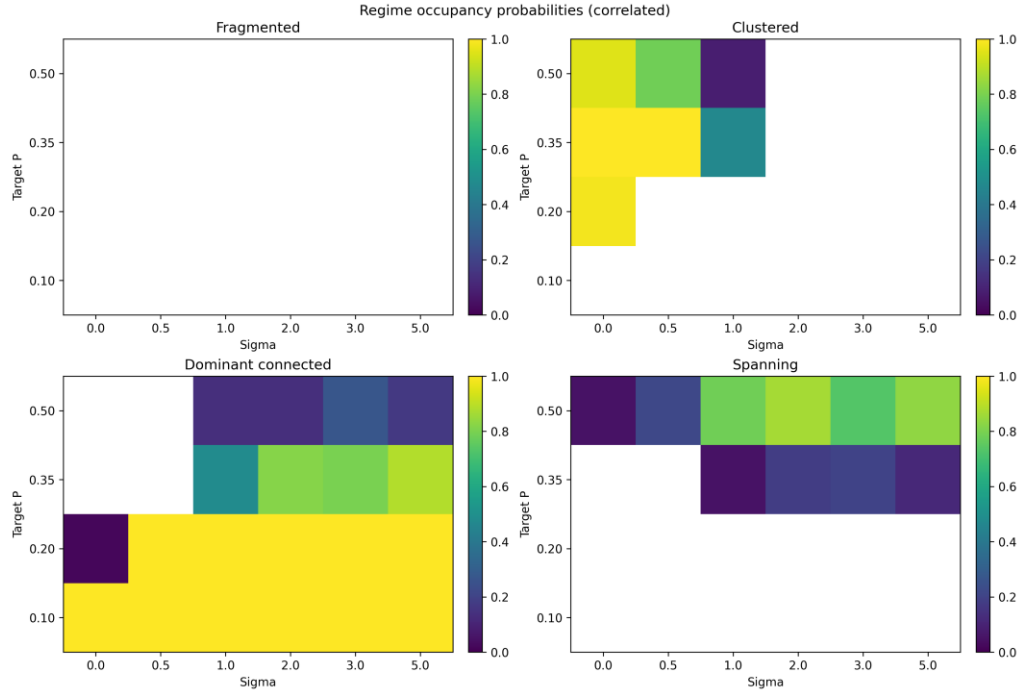

Figure 13: Regime-occupancy probabilities for the correlated ensemble. Each panel shows the probability that a realization belongs to a given connectivity regime under each coherence–occupation combination.

This regime-occupancy structure provides a stronger interpretation of non-uniqueness than ensemble averages alone. Equal probability fixes the occupied fraction, but correlation determines which connected-state classes remain accessible. The transition zone is therefore better interpreted as a region of competing accessible states rather than as a simple crossover in average connectivity metrics.

4.5. Mesoscale aggregation and fluctuation peaks

The fragmentation-to-spanning evolution is not captured fully by the largest connected component alone. To resolve the intermediate stage of structural consolidation, the second-largest cluster fraction S2 and the mean finite-cluster size were examined as mesoscale indicators. These quantities are useful because they track whether occupied mass is being transferred directly into a single dominant component or temporarily distributed among competing intermediate-scale structures.

Figure 14 shows that the mean S2 fraction generally increases from low to intermediate coherence before stabilizing or declining, depending on the target occupation probability. This pattern indicates that, during the transition, the system may contain more than one large connected structure. In other words, occupied mass is first redistributed into competing mesoscale clusters before final consolidation into a dominant or spanning component.

https://doi.org/10.5194/egusphere-2026-2387
Preprint. Discussion started: 17 June 2026

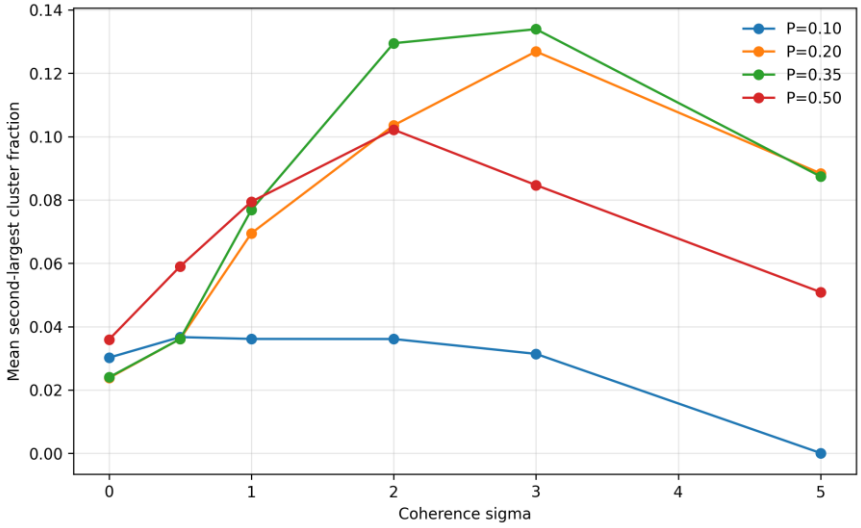

425 **Figure 14: Mean second-largest cluster fraction S2 across coherence levels for different target occupation probabilities.**

The mean finite-cluster size provides complementary evidence for the same process **(Figure 15).** Its increase at intermediate coherence levels indicates that non-dominant clusters can grow substantially before being absorbed into larger connected structures or losing relative importance. This supports a multi-stage interpretation of the transition: fragmentation is first reduced through mesoscale aggregation, and only later does large-scale consolidation become dominant.

430

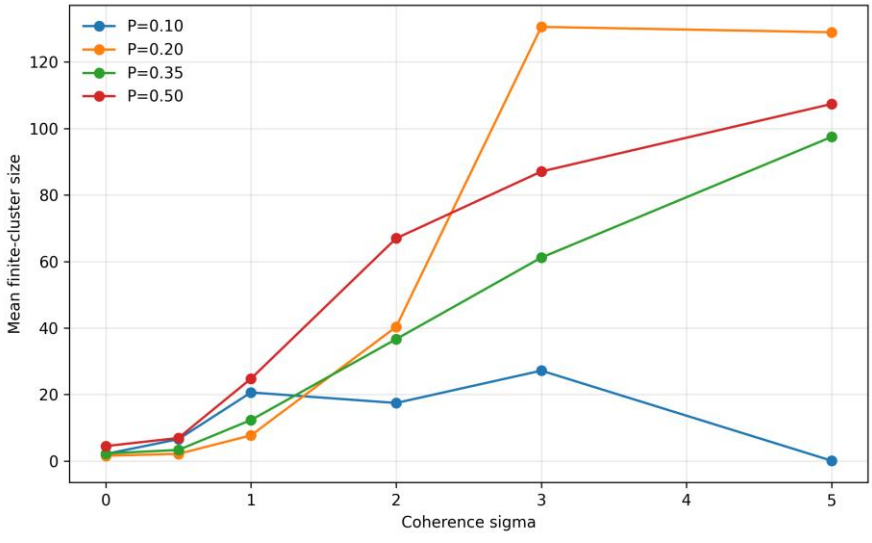

Figure 15. Mean finite-cluster size across coherence levels for different target occupation probabilities.

https://doi.org/10.5194/egusphere-2026-2387
Preprint. Discussion started: 17 June 2026

The fluctuation landscape further clarifies that this transition is distributed across multiple structural scales. **Figure 16** shows heatmaps of Var(Γ), Var(Nc), Var(spanning), and mean susceptibility across coherence–occupation conditions. These descriptors do not peak in the same regions of parameter space. Variability in Nc is strongest near low coherence, reflecting sensitivity in highly partitioned configurations, whereas Γ, spanning, susceptibility, and S2 respond more strongly in intermediate or higher coherence ranges.

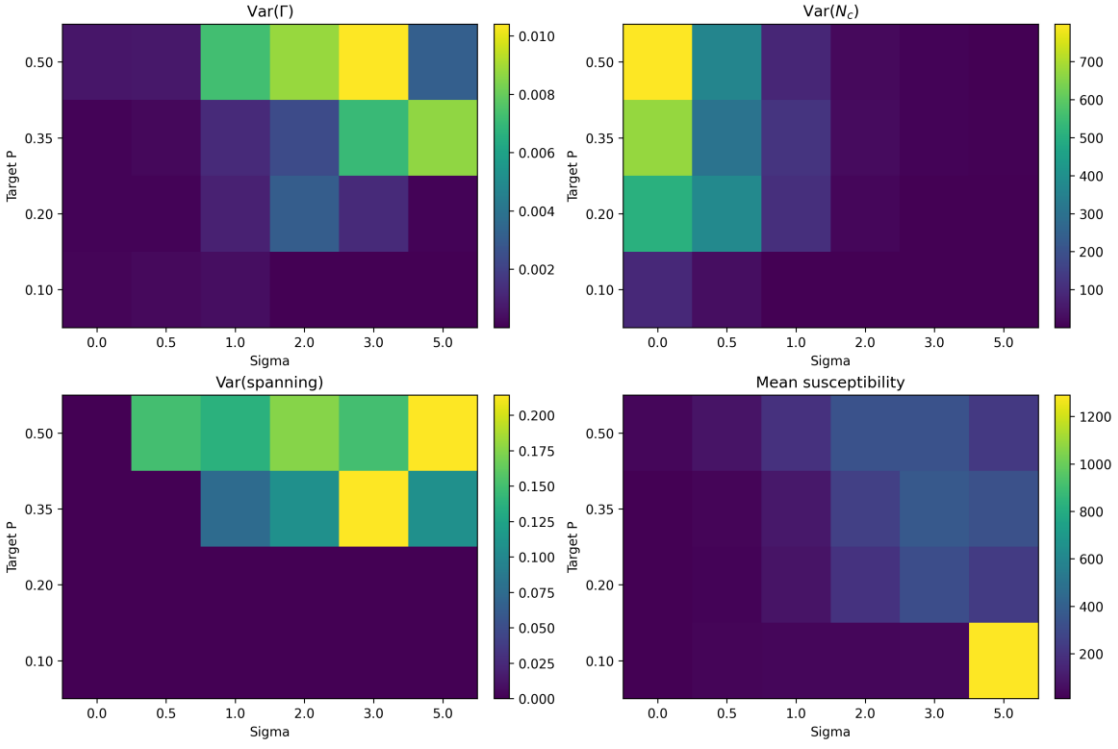

Figure 16: Fluctuation heatmaps for Var(Γ), Var(Nc), Var(Pspanning), and mean susceptibility across coherence and target occupation conditions.

This scale-dependent behavior is summarized in **Figure 17**, which shows the coherence levels at which the main fluctuation and mesoscale metrics attain their peak values. The fact that these peaks occur at different coherence levels indicates that the transition does not collapse to a single critical coherence threshold. Instead, fragmentation sensitivity, mesoscale aggregation, dominant-cluster variability, and spanning variability represent different stages of the same reorganization process.

https://doi.org/10.5194/egusphere-2026-2387
Preprint. Discussion started: 17 June 2026

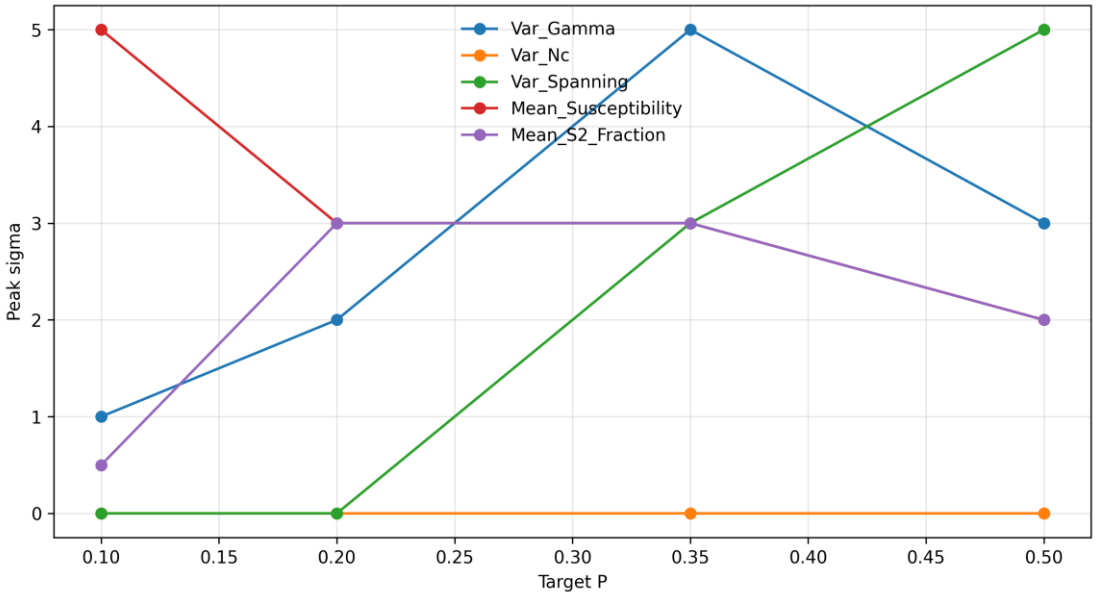

Figure 17: Peak coherence locations of fluctuation and mesoscale metrics across target occupation levels.

Taken together, Figures 14–17 show that the fragmentation-to-spanning evolution is a multi-stage reorganization process. The system first develops competing mesoscale structures, then progressively concentrates occupied mass into dominant or spanning configurations. This interpretation complements the regime-occupancy results by showing that state multiplicity is accompanied by scale-dependent redistribution of connected mass.

4.6. Robustness of the connectivity transition framework

Additional sensitivity analyses were conducted to evaluate whether the proposed connectivity-based interpretation remains stable under alternative analytical choices. These analyses considered neighborhood definition, spanning criterion, stochastic perturbation intensity, regime-threshold calibration, and observed-versus-simulated structural correspondence. The purpose was not to redefine the main results, but to assess whether the coherence-driven transition remains interpretable beyond a single modeling convention.

First, the neighborhood definition was varied by comparing 4-neighbor and 8-neighbor connectivity rules. Although the absolute values of some descriptors changed, especially those related to local adjacency and component partitioning, the dominant-cluster ratio followed the same increasing trend with coherence under both definitions (**Figure 18**). This indicates that the main consolidation pattern is not an artifact of a single neighborhood convention.

https://doi.org/10.5194/egusphere-2026-2387
Preprint. Discussion started: 17 June 2026

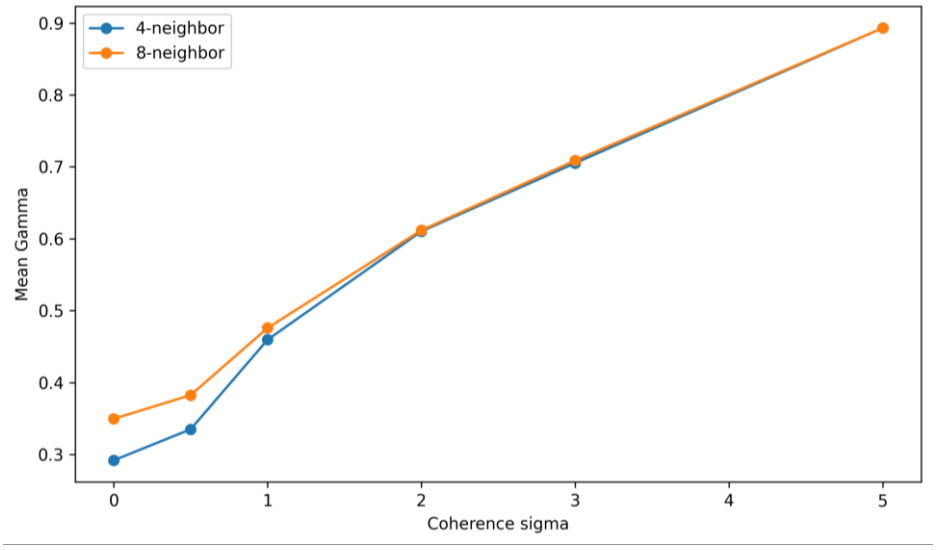

Figure 18: Neighborhood sensitivity of the dominant-cluster ratio under 4-neighbor and 8-neighbor connectivity definitions.

The spanning criterion was then tested using left-right, top-bottom, and either-direction definitions. As expected, the either-direction criterion produced the most permissive classification, whereas the stricter directional definitions yielded lower spanning probabilities **(Figure 19)**. The left-right criterion was therefore retained in the main analysis because it provides a conservative basis for identifying domain-scale continuity and avoids over-classifying partially connected structures as spanning.

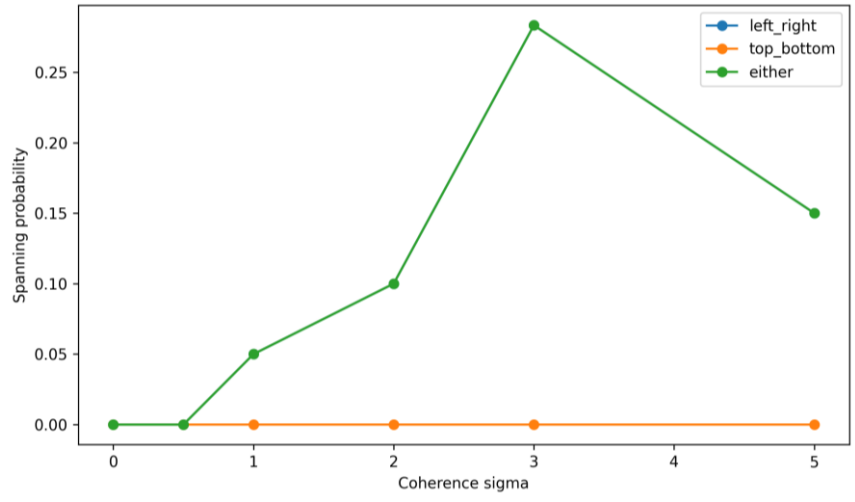

Figure 19: Sensitivity of spanning probability under alternative spanning criteria, including left-right, top-bottom, and either-direction definitions.

https://doi.org/10.5194/egusphere-2026-2387
Preprint. Discussion started: 17 June 2026

The sensitivity to stochastic perturbation intensity was also evaluated using the susceptibility-like finite-cluster measure. Although the absolute magnitude of susceptibility varies with the imposed noise level, the main response remains concentrated around intermediate coherence levels (**Figure 20)**. This indicates that the mesoscale finite-cluster signal is not solely an artifact of a single perturbation amplitude, even though its amplitude is noise-sensitive.

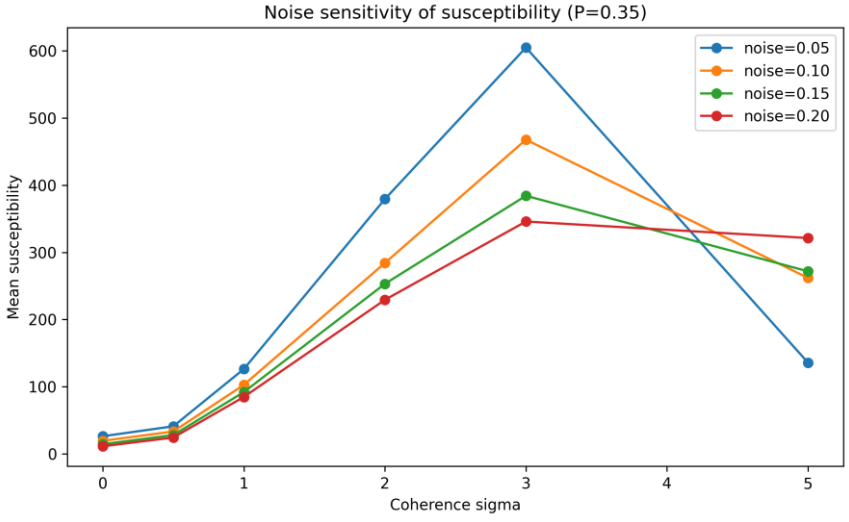

Figure 20: Noise sensitivity of the susceptibility-like finite-cluster response for P=0.35.

The robustness of the regime classification was examined using alternative threshold sets for fragmented, clustered, dominant-connected, and spanning states. Although some local classifications shifted under stricter or looser thresholds, the broader topology of the regime map remained stable, particularly in distinguishing low-coherence clustered behavior from higher-coherence dominant or spanning states (**Figure 21**). This shows that the regime interpretation is not purely threshold-driven, even if some boundary cells remain sensitive to calibration choices.

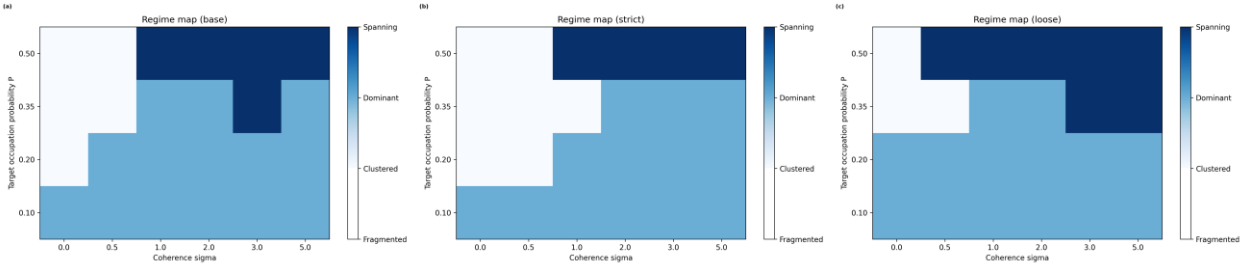

Figure 21: Regime maps obtained under alternative threshold calibrations for fragmented, clustered, dominant connected, and spanning states.

https://doi.org/10.5194/egusphere-2026-2387
Preprint. Discussion started: 17 June 2026

Finally, the relationship between the observed manifestation field and the controlled ensemble was evaluated using structural similarity measures. The purpose was not to reproduce the observed field exactly, but to verify that the simulated fields remained linked to the observed organizational template. The similarity results indicate partial structural correspondence across selected coherence–occupation conditions (**Figure 22**). This supports the use of the observed field as an empirical anchor, while confirming that the controlled ensemble should be interpreted as a mechanism-oriented experiment rather than as a deterministic reconstruction of the observed pattern.

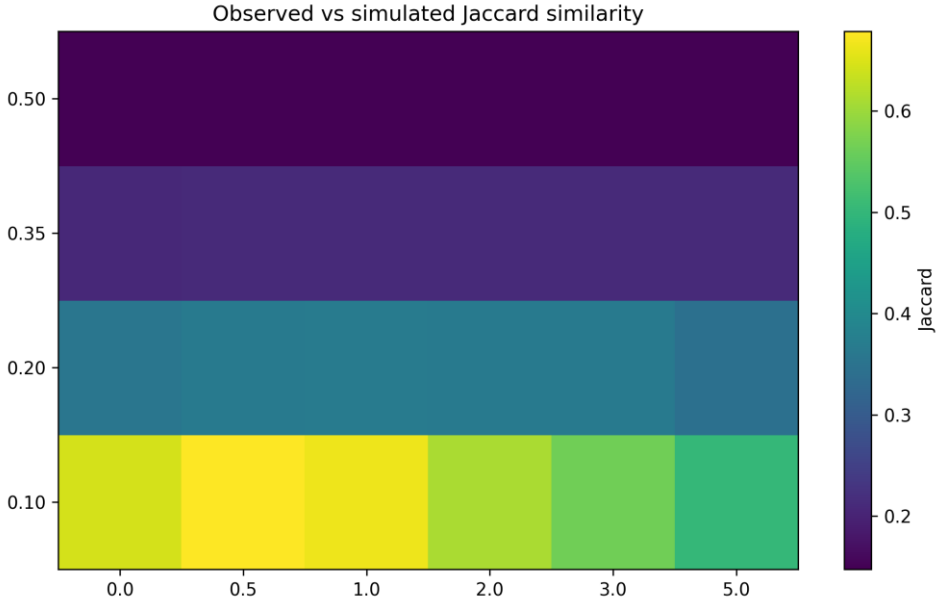

Figure 22: Observed-versus-simulated structural similarity across coherence and occupation conditions.

Overall, the robustness analyses support the interpretation of the fragmentation-to-spanning evolution as a genuine connectivity transition rather than a numerical artifact of a particular analytical setup. The main conclusion remains stable across alternative neighborhood rules, spanning definitions, perturbation amplitudes, and threshold calibrations: equal-probability fields do not define a unique connected state, and spatial coherence reorganizes the occupied domain from partitioned local structures toward larger-scale connected configurations.

5. Discussion

5.1. Organizational meaning of equal-probability non-uniqueness

Equal probability is not sufficient to define the collective state of a correlated hazard field. Fields constructed under the same prescribed occupation level may nevertheless display markedly different connectivity structures, ranging from partitioned

https://doi.org/10.5194/egusphere-2026-2387
Preprint. Discussion started: 17 June 2026

local arrangements to dominant connected domains and spanning states. The main implication is that abundance alone does not uniquely determine organization. Scalar quantities such as occupied fraction or exceedance ratio describe the extent of activation, but not whether the active domain remains dispersed, aggregates into clusters, concentrates into a dominant component, or develops domain-scale continuity. The proposed framework therefore separates two complementary dimensions of system state: how much of the domain is active and how that activity is spatially organized (Cross & Hohenberg, 1993; Turcotte, 1999).

This distinction clarifies the meaning of the regime structure identified in the study. Fragmented, clustered, dominant-connected, and spanning configurations should not be interpreted as visual variants of the same scalar condition. They represent distinct connected-state classes within an equal-probability ensemble. Fragmented states correspond to partitioned activation, clustered states to partial aggregation, dominant-connected states to concentration into a major component, and spanning states to domain-scale continuity. The regime distribution across realizations therefore provides a system-level description of how different organizational states remain accessible under a given coherence–occupation constraint (Vicsek & Zafeiris, 2012).

The null-model comparison sharpens this conclusion. Equal-probability fields without imposed coherence remain effectively fragmented, whereas correlated fields access clustered, dominant-connected, and spanning states under the same scalar constraints. Non-uniqueness should therefore be interpreted not merely as variability in descriptor values, but as a coherence-dependent expansion of the accessible connected-state space. In this sense, spatial correlation changes not only the mean structure of the field, but also the range of organizational states available to it.

5.2. Transition structure, robustness, and interpretive limits

The results are most naturally interpreted as a coherence-driven connectivity transition in a correlated threshold system. As spatial coherence increases, the field does not merely become smoother; it reorganizes the occupied domain into larger and more coherent connected structures. This transition is not characterized by a single sharp boundary. Instead, intermediate coherence ranges form transition bands in which clustered, dominant-connected, and near-spanning configurations can coexist under identical scalar constraints. The system therefore passes through regions of elevated organizational variability before more consolidated states become dominant.

The second-largest cluster and fluctuation-peak analyses refine this interpretation by showing that the transition has a mesoscale component. The system does not move directly from many small disconnected clusters to one dominant connected domain. Rather, occupied mass is first redistributed among competing intermediate-scale structures, which may later merge into dominant or spanning configurations. This supports a multi-stage interpretation of fragmentation-to-spanning behavior: local partitioning is reduced first, mesoscale competition emerges next, and large-scale consolidation follows under sufficient coherence and occupation.

The robustness analyses help define the limits of interpretation without weakening the main conclusion. The observed manifestation field should be understood as an empirical anchor, not as a deterministic target that the controlled ensemble is

https://doi.org/10.5194/egusphere-2026-2387
Preprint. Discussion started: 17 June 2026

expected to reproduce exactly. Its role is to provide a real-data-informed organizational reference from which the latent template is derived. Similarly, the regime thresholds should not be interpreted as universal constants. Alternative threshold calibrations can shift some local regime boundaries, especially near intermediate coherence conditions where organizational competition is strongest. However, these shifts do not alter the broader topology of the coherence–occupation space or the central conclusion that equal-probability fields are non-unique at the system level (Saltelli et al., 2008).

A further implication is that interpretive uncertainty is not uniform across the regime sequence. Fragmented and weakly clustered states are more sensitive to neighborhood rule, grid resolution, and local connectivity convention because they are controlled by many small components. By contrast, once large-scale connectedness emerges, dominant and near-spanning structures become more stable and less dependent on local analytical choices. Spanning probabilities may still vary near the transition zone, but the existence of high-coherence, high-connectivity states remains structurally persistent. The main interpretive uncertainty is therefore concentrated at the fragmented end of the sequence and within the transition band, rather than across the full parameter space (Helton et al., 2006).

5.3. Broader relevance for complexity-oriented hazard analysis

The broader significance of the study lies in its contribution to complexity-oriented hazard interpretation. Hazard fields are often read primarily through scalar extent measures, such as damaged fraction, exceedance area, or marginal failure probability. The present results show that this perspective is incomplete because fields with similar extent may still imply fundamentally different system-scale organizations. A dispersed set of local clusters and a dominant connected domain are not equivalent simply because they occupy comparable fractions of space. Connectivity-based descriptors therefore provide a second interpretive layer that reveals whether the active system remains partitioned, becomes hierarchically aggregated, or reaches domain-scale continuity. This shifts the analysis from local-event counting toward collective-state interpretation (Mitchell, 2009; Holland, 2014).

From a complexity perspective, the null-model contrast is especially informative. It shows that equal occupation constrains abundance, but not the connected-state space accessible to the system. The correlated ensemble does not merely produce different values of the same descriptors; it makes different organizational regimes available under stochastic realization. This distinction between scalar extent and accessible connected-state space is one of the main theoretical implications of the present study and helps situate the results within broader interpretations of correlated threshold fields.

Although the motivating example is a liquefaction manifestation field, the contribution of the study is not limited to the geotechnical setting. The same logic applies to a wider class of correlated threshold systems in which local activation can reorganize into connected collective structure. In that sense, the framework is better understood as a general organizational approach to thresholded correlated fields than as a domain-specific hazard tool alone. Its value is to show that equal-probability fields are non-unique at the system level and that this non-uniqueness can be studied systematically through connected-state classes, transition bands, and large-scale restructuring. This provides a bridge between correlated random

https://doi.org/10.5194/egusphere-2026-2387
Preprint. Discussion started: 17 June 2026

fields, thresholded spatial organization, and the broader complexity-science language of emergence, regime change, and collective structure (Goldenfeld & Kadanoff, 1999).

6. Conclusions

This study examined equal-probability hazard fields as correlated threshold systems whose large-scale organization cannot be inferred from marginal occupation probability alone. Using an observed liquefaction manifestation field as an empirical anchor, a controlled coherence-based ensemble was constructed and thresholded under exact equal-probability conditions. This design made it possible to separate activation extent from spatial arrangement and to test whether fields with the same occupied fraction can nevertheless occupy different connected states.

The results show that equal probability constrains activation extent, but not connected organization. Fields with the same prescribed occupation level may range from partitioned local clusters to dominant connected domains and system-spanning configurations, depending on the imposed spatial coherence. Increasing coherence reorganizes the occupied domain by reducing connected-component count, increasing the dominant-cluster ratio, concentrating occupied mass within the largest components, and, under favorable occupation conditions, enabling spanning continuity. Thus, coherence does not merely smooth the underlying field; it changes the collective organization of the thresholded system.

The cluster-size hierarchy, second-largest-cluster response, and finite-cluster susceptibility further show that the transition proceeds through hierarchical and mesoscale aggregation. The system does not move directly from many isolated small clusters to one dominant connected component. Instead, occupied mass is first redistributed among competing intermediate-scale structures before large-scale consolidation becomes dominant. This finding is important because it shows that the fragmentation-to-spanning evolution is not only a change in the largest component, but a scale-dependent redistribution of connected mass across the full cluster hierarchy.

The fluctuation and regime analyses indicate that the fragmentation-to-spanning evolution is not governed by a single sharp threshold. Intermediate coherence ranges form transition bands in which competing organizational outcomes coexist under identical scalar constraints. Regime-occupancy probabilities show that equal-probability fields are better interpreted as distributions over accessible connected-state classes than as perturbations around a single deterministic state. In this sense, non-uniqueness is not random scatter around one expected pattern, but a structured property of the coherence–occupation state space.

The null-model comparison confirms that the observed transition sequence is correlation-driven. Under the same occupation constraints, uncorrelated fields remain effectively fragmented, whereas correlated fields access clustered, dominant-connected, and spanning regimes. Sensitivity analyses further show that local classifications can vary with neighborhood definition, spanning criterion, perturbation amplitude, and regime-threshold calibration, but the broader coherence-driven reorganization remains structurally interpretable. The observed manifestation field should therefore be understood as an empirical anchor for the framework, not as a deterministic target for exact spatial reproduction.

https://doi.org/10.5194/egusphere-2026-2387
Preprint. Discussion started: 17 June 2026

The main conclusions are as follows:

Equal-probability hazard fields are organizationally non-unique; identical occupation levels may correspond to different connectivity states.

Connectivity provides a system-level descriptor that complements scalar probability by distinguishing activation extent from spatial arrangement.

Fragmented, clustered, dominant-connected, and spanning configurations represent distinct connected-state classes rather than visual variants of the same field.

The fragmentation-to-spanning evolution is governed jointly by occupation level and spatial coherence and unfolds through transition bands characterized by elevated variability and competing outcomes.

Null-model comparisons show that correlation is required for access to clustered, dominant-connected, and spanning states under fixed occupation constraints.

Second-largest-cluster and fluctuation-peak analyses indicate that the transition proceeds through mesoscale aggregation and scale-dependent redistribution of connected mass.

The proposed framework supports a complexity-oriented interpretation of hazard fields as spatial systems capable of occupying distinct collective states, rather than as maps of local exceedance alone.

Although motivated by a liquefaction manifestation field, the framework is not limited to geotechnical hazards. It provides a general organizational approach for thresholded correlated fields in which local activation may reorganize into collective connected structure. Future work may extend the framework to anisotropic coherence structures, three-dimensional domains, alternative interaction topologies, and other correlated threshold systems. Such extensions would help clarify how geometry, correlation structure, and interaction topology influence the location, breadth, and stability of connectivity-transition bands.

Code and data availability.

The scripts and derived data used to reproduce the analyses and figures will be made available in a public repository upon acceptance. The original observational data are not redistributed in raw form, but processed data and figure source files are available to reviewers upon request.

Author contributions

SCT conceived the study, designed the computational framework, processed the data, developed the analysis scripts, performed the simulations, interpreted the results, prepared the figures, and wrote the manuscript.

Competing interests

The author declares that there are no competing interests.

https://doi.org/10.5194/egusphere-2026-2387
Preprint. Discussion started: 17 June 2026

Acknowledgements

The author acknowledges the open-source scientific Python ecosystem used for numerical computation, spatial analysis, and visualization in this study.

Financial support

This research received no external funding.

References

Achlioptas, D., D'Souza, R. M., and Spencer, J.: Explosive percolation in random networks, Science, 323, 1453–1455, https://doi.org/10.1126/science.1167782, 2009.

Balberg, I., Anderson, C. H., Alexander, S., and Wagner, N.: Excluded volume and its relation to the onset of percolation, Phys. Rev. B, 30, 3933–3943, https://doi.org/10.1103/PhysRevB.30.3933, 1984.

Barabási, A. L. and Albert, R.: Emergence of scaling in random networks, Science, 286, 509–512, https://doi.org/10.1126/science.286.5439.509, 1999.

Barthélemy, M.: Spatial networks, Phys. Rep., 499, 1–101, https://doi.org/10.1016/j.physrep.2010.11.002, 2011.

Binder, K.: Finite size scaling analysis of Ising model block distribution functions, Z. Phys. B Condens. Matter, 43, 119–140, https://doi.org/10.1007/BF01293604, 1981.

Callaway, D. S., Newman, M. E. J., Strogatz, S. H., and Watts, D. J.: Network robustness and fragility: percolation on random graphs, Phys. Rev. Lett., 85, 5468–5471, https://doi.org/10.1103/PhysRevLett.85.5468, 2000.

Clauset, A., Shalizi, C. R., and Newman, M. E. J.: Power-law distributions in empirical data, SIAM Rev., 51, 661–703, https://doi.org/10.1137/070710111, 2009.

Christensen, K. and Moloney, N. R.: Complexity and Criticality, Imperial College Press, London, UK, 2005.

Cohen, R., Erez, K., Ben-Avraham, D., and Havlin, S.: Resilience of the Internet to random breakdowns, Phys. Rev. Lett., 85, 4626–4628, https://doi.org/10.1103/PhysRevLett.85.4626, 2000.

Cressie, N.: Statistics for Spatial Data, Wiley, New York, USA, 1993.

Cross, M. C. and Hohenberg, P. C.: Pattern formation outside of equilibrium, Rev. Mod. Phys., 65, 851–1112, https://doi.org/10.1103/RevModPhys.65.851, 1993.

Dorogovtsev, S. N., Mendes, J. F. F., and Samukhin, A. N.: Giant strongly connected component of directed networks, Phys. Rev. E, 64, 025101, https://doi.org/10.1103/PhysRevE.64.025101, 2001.

Fenton, G. A.: Random field modeling of CPT data, J. Geotech. Geoenviron. Eng., 125, 486–498, https://doi.org/10.1061/(ASCE)1090-0241(1999)125:6(486), 1999.

https://doi.org/10.5194/egusphere-2026-2387
Preprint. Discussion started: 17 June 2026

Fishman, G. S.: Monte Carlo: Concepts, Algorithms, and Applications, Springer, New York, USA, 1996.

Ghanbarian, B., Hunt, A. G., Ewing, R. P., and Sahimi, M.: Tortuosity in porous media: a critical review, Soil Sci. Soc. Am. J., 77, 1461–1477, https://doi.org/10.2136/sssaj2012.0435, 2013.

Goldenfeld, N.: Lectures on Phase Transitions and the Renormalization Group, CRC Press, Boca Raton, USA, https://doi.org/10.1201/9780429493492, 2018.

Goldenfeld, N. and Kadanoff, L. P.: Simple lessons from complexity, Science, 284, 87–89, https://doi.org/10.1126/science.284.5411.87, 1999.

Goda, K. and Atkinson, G. M.: Intraevent spatial correlation of ground-motion parameters using SK-net data, Bull. Seismol. Soc. Am., 100, 3055–3067, https://doi.org/10.1785/0120100031, 2010.

He, F. and Hubbell, S. P.: Percolation theory for the distribution and abundance of species, Phys. Rev. Lett., 91, 198103, https://doi.org/10.1103/PhysRevLett.91.198103, 2003.

Helton, J. C., Johnson, J. D., Sallaberry, C. J., and Storlie, C. B.: Survey of sampling-based methods for uncertainty and sensitivity analysis, Reliab. Eng. Syst. Saf., 91, 1175–1209, https://doi.org/10.1016/j.ress.2005.11.017, 2006.

Holland, J. H.: Complexity: A Very Short Introduction, Oxford University Press, Oxford, UK, 2014.

Hoshen, J. and Kopelman, R.: Percolation and cluster distribution. I. Cluster multiple labeling technique and critical concentration algorithm, Phys. Rev. B, 14, 3438–3445, https://doi.org/10.1103/PhysRevB.14.3438, 1976.

Jayaram, N. and Baker, J. W.: Correlation model for spatially distributed ground-motion intensities, Earthq. Eng. Struct. Dyn., 38, 1687–1708, https://doi.org/10.1002/eqe.922, 2009.

Keitt, T. H., Urban, D. L., and Milne, B. T.: Detecting critical scales in fragmented landscapes, Conserv. Ecol., 1, 4, 1997.

Kelso, J. A. S.: Dynamic Patterns: The Self-Organization of Brain and Behavior, MIT Press, Cambridge, USA, 1995.

Mitchell, M.: Complexity: A Guided Tour, Oxford University Press, Oxford, UK, 2009.

Morowitz, H. J.: The Emergence of Everything: How the World Became Complex, Oxford University Press, Oxford, UK, 2002.

Muñoz, M. A.: Colloquium: Criticality and dynamical scaling in living systems, Rev. Mod. Phys., 90, 031001, https://doi.org/10.1103/RevModPhys.90.031001, 2018.

Newman, M. E. J.: Spread of epidemic disease on networks, Phys. Rev. E, 66, 016128, https://doi.org/10.1103/PhysRevE.66.016128, 2002.

Newman, M. E. J. and Ziff, R. M.: Fast Monte Carlo algorithm for site or bond percolation, Phys. Rev. E, 64, 016706, https://doi.org/10.1103/PhysRevE.64.016706, 2001.

Pascual, M. and Guichard, F.: Criticality and disturbance in spatial ecological systems, Trends Ecol. Evol., 20, 88–95, https://doi.org/10.1016/j.tree.2004.11.012, 2005.

Rozenfeld, H. D., Rybski, D., Andrade, J. S., Batty, M., Stanley, H. E., and Makse, H. A.: Laws of population growth, Proc. Natl. Acad. Sci. USA, 105, 18702–18707, https://doi.org/10.1073/pnas.0807435105, 2008.

https://doi.org/10.5194/egusphere-2026-2387
Preprint. Discussion started: 17 June 2026

Saberi, A. A.: Recent advances in percolation theory and its applications, Phys. Rep., 578, 1–32, https://doi.org/10.1016/j.physrep.2015.03.003, 2015.

Sahimi, M.: Applications of Percolation Theory, Taylor & Francis, London, UK, https://doi.org/10.1201/9781482272444, 1994.

Saltelli, A., Ratto, M., Andres, T., Campolongo, F., Cariboni, J., Gatelli, D., Saisana, M., and Tarantola, S.: Global Sensitivity Analysis: The Primer, Wiley, Chichester, UK, 2008.

Schrenk, K. J., Araújo, N. A. M., Andrade, J. S., and Herrmann, H. J.: Fracturing ranked surfaces, Sci. Rep., 2, 348, https://doi.org/10.1038/srep00348, 2012.

Schläpfer, M., Bettencourt, L. M. A., Grauwin, S., Raschke, M., Claxton, R., Smoreda, Z., West, G. B., and Ratti, C.: The scaling of human interactions with city size, J. R. Soc. Interface, 11, 20130789, https://doi.org/10.1098/rsif.2013.0789, 2014.

Scheffer, M., Bascompte, J., Brock, W. A., Brovkin, V., Carpenter, S. R., Dakos, V., Held, H., van Nes, E. H., Rietkerk, M., and Sugihara, G.: Early-warning signals for critical transitions, Nature, 461, 53–59, https://doi.org/10.1038/nature08227, 2009.

Shinozuka, M. and Deodatis, G.: Simulation of multi-dimensional Gaussian stochastic fields by spectral representation, Appl. Mech. Rev., 49, 29–53, https://doi.org/10.1115/1.3101883, 1996.

Stanley, H. E.: Scaling, universality, and renormalization: three pillars of modern critical phenomena, Rev. Mod. Phys., 71, S358–S366, https://doi.org/10.1103/RevModPhys.71.S358, 1999.

Stauffer, D.: Scaling theory of percolation clusters, Phys. Rep., 54, 1–74, https://doi.org/10.1016/0370-1573(79)90060-7, 1979.

Stein, M. L.: Interpolation of Spatial Data: Some Theory for Kriging, Springer, New York, USA, 1999.

Turner, M. G.: Landscape ecology: the effect of pattern on process, Annu. Rev. Ecol. Syst., 20, 171–197, https://doi.org/10.1146/annurev.es.20.110189.001131, 1989.

Torquato, S.: Hyperuniform states of matter, Phys. Rep., 745, 1–95, https://doi.org/10.1016/j.physrep.2018.03.001, 2018.

Turcotte, D. L.: Self-organized criticality, Rep. Prog. Phys., 62, 1377–1429, https://doi.org/10.1088/0034-4885/62/10/201, 1999.

Urban, D. L., Minor, E. S., Treml, E. A., and Schick, R. S.: Graph models of habitat mosaics, Ecol. Lett., 12, 260–273, https://doi.org/10.1111/j.1461-0248.2008.01271.x, 2009.

Vicsek, T. and Zafeiris, A.: Collective motion, Phys. Rep., 517, 71–140, https://doi.org/10.1016/j.physrep.2012.03.004, 2012.

Wang, M. and Takada, T.: Macrospatial correlation model of seismic ground motions, Earthq. Spectra, 21, 1137–1156, https://doi.org/10.1193/1.2083887, 2005.

With, K. A., Gardner, R. H., and Turner, M. G.: Landscape connectivity and population distributions in heterogeneous environments, Oikos, 78, 151–169, https://doi.org/10.2307/3545811, 1997.

https://doi.org/10.5194/egusphere-2026-2387
Preprint. Discussion started: 17 June 2026

740 Ziff, R. M.: Spanning probability in 2D percolation, Phys. Rev. Lett., 69, 2670–2673, https://doi.org/10.1103/PhysRevLett.69.2670, 1992.

Ziff, R. M.: Scaling behavior of explosive percolation on the square lattice, Phys. Rev. E, 82, 051105, https://doi.org/10.1103/PhysRevE.82.051105, 2010.

745